

# Methanol Selective Oxidation to Methyl Formate over $\text{ReO}_x/\text{CeO}_2$ Catalysts

Junlong Liu · Ensheng Zhan · Weijie Cai ·  
Juan Li · Wenjie Shen

Received: 22 July 2007 / Accepted: 13 September 2007 / Published online: 16 October 2007  
© Springer Science+Business Media, LLC 2007

**Abstract** Methanol selective oxidation to methyl formate was investigated over  $\text{ReO}_x/\text{CeO}_2$  catalysts in terms of Re loading and reaction mechanism. It was found that Re loading with monolayer dispersion on ceria exhibited promising reaction rate of methanol of  $16 \text{ mmol g}_{\text{cat}}^{-1} \text{ h}^{-1}$  and methyl formate selectivity of about 90% at 513 K. The surface reaction of methanol, formaldehyde, and methyl formate over the  $\text{ReO}_x/\text{CeO}_2$  catalyst was investigated by in situ Fourier transform infrared spectroscopy and it was revealed that the formate species, formed by the oxidation of adsorbed  $-\text{OCH}_3$  species, could act as the key reaction intermediate, which further reacted with gaseous methanol to form methyl formate and/or decompose into CO and  $\text{CO}_2$ , depending on the reaction temperature.

**Keywords** Methanol · Selective oxidation · Methyl formate ·  $\text{ReO}_x/\text{CeO}_2$  · FT-IR

## 1 Introduction

Methyl formate is one of the most important building block molecules in  $\text{C}_1$  chemistry, which can be used to synthesize formic acid, dimethyl carbonate, and acetic acid. Methyl formate is currently produced by carbonylation of methanol in liquid phase using sodium methoxide as catalyst [1]. However, the alkali methoxide catalysts are extremely sensitive to minute contaminants, particularly moisture and  $\text{CO}_2$ , which often caused operation problems like easy deactivation and difficult separation. Dehydrogenation of

methanol over Cu-based catalysts is regarded as an alternative route to produce methyl formate, but the conversion of methanol is limited by thermodynamic equilibrium and the decomposition of methyl formate became the main reaction at temperature higher than 623 K [2–4].

Alternatively, selective oxidation of methanol to methyl formate is proposed as a favorable reaction.  $\text{V}_2\text{O}_5/\text{TiO}_2$  [5–6] and  $\text{MoO}_3/\text{SnO}_2$  [7] catalysts have been demonstrated to be effective for this process, but higher selectivity of methyl formate was obtained only in a very narrow temperature window. For example, the most promising result with 72% conversion of methanol and 90% selectivity of methyl formate was achieved over a  $\text{MoO}_3/\text{SnO}_2$  catalyst at 433 K [7]. However, the specific yield of methyl formate was only  $1.9 \text{ mmol g}_{\text{cat}}^{-1} \text{ h}^{-1}$ , which is still very low when compared with the industrial values.

In this work, we report effective  $\text{ReO}_x/\text{CeO}_2$  catalysts for selective oxidation of methanol to methyl formate, over which rather high methanol conversion and methyl formate selectivity have been obtained under very mild conditions. The effect of Re loading on the catalytic performance and the reaction mechanism were extensively studied.

## 2 Experimental

### 2.1 Catalyst Preparation

The  $\text{ReO}_x/\text{CeO}_2$  catalysts with Re loading of 2.9–16.8 wt.% were prepared by incipient-wetness impregnation of a commercial  $\text{CeO}_2$  (BET surface area of  $93 \text{ m}^2 \text{ g}^{-1}$ ) with aqueous solution of  $\text{NH}_4\text{ReO}_4$ . Desirable amounts of  $\text{NH}_4\text{ReO}_4$  were dissolved into equal amount of  $\text{H}_2\text{O}$  which was then used to wet the  $\text{CeO}_2$  powder. The samples were dried at 383 K overnight and finally calcined at 673 K for 6 h in air.

J. Liu · E. Zhan · W. Cai · J. Li · W. Shen (✉)  
State Key Laboratory of Catalysis, Dalian Institute of Chemical  
Physics, Chinese Academy of Sciences, Dalian 116023, China  
e-mail: shen98@dicp.ac.cn

## 2.2 Catalysts Characterization

The actual Re loading of the catalysts were obtained by inductively coupled plasma atomic emission spectroscopy (ICP-AES) on a Plasam-Spec-I spectrometer.

N<sub>2</sub> adsorption–desorption isotherms were obtained at 77 K using a Micrometrics ASAP 2010 analyzer. Prior to measurement, the samples were degassed at 572 K for 2 h. The surface area was calculated from a multipoint BET analysis of nitrogen adsorption isotherm.

X-ray power diffraction (XRD) patterns were recorded on a D/MAX 2500 X-Ray diffractometer (Rigaku), using Cu-K $\alpha$  radiation operated at 40 kV and 100 mA.

Temperature-programmed reduction (TPR) was conducted with a conventional apparatus equipped with a thermal conductivity detector. In a typical run, 20 mg samples were loaded and heated to 573 K (10 K min<sup>-1</sup>) under N<sub>2</sub> flow (30 ml min<sup>-1</sup>) and kept at this temperature for 0.5 h to remove the adsorbed carbonates and hydrates. After cooling down to room temperature and introducing the reduction agent of 5% H<sub>2</sub>/N<sub>2</sub> (30 ml min<sup>-1</sup>), the temperature was then programmed to rise at a ramp of 10 K min<sup>-1</sup>.

## 2.3 In situ FT-IR

The in situ IR spectra were recorded on a Bruker vector–22 FTIR spectrometer with a resolution of 2 cm<sup>-1</sup> using 64 scans. The IR was operated in absorbance mode using a high temperature and pressure cell with ZnSe windows. The sample was pressed into self-supporting wafer and mounted into the IR cell. It was then purged with He at 673 K for 4 h to eliminate the surface impurities. The spectra of the clean sample were then recorded at different temperature as background under He flow. The IR measurement was carried out by introducing saturated methanol (11 vol.%), methyl formate (13 vol.%), and formaldehyde (10 vol.%) in He. The adsorption of individual component was measured at room temperature, and then the saturated adsorbed catalyst was heated in flow of He. The reference of spectrum of the ReO<sub>x</sub>/CeO<sub>2</sub> wafer in He taken at the measurement temperature was subtracted from each spectrum.

## 2.4 Catalytic Evaluation

The selective oxidation of methanol was carried out in a fixed-bed quartz flow reactor under atmospheric pressure. About 100 mg catalysts (40–60 mesh) were diluted with 150 mg quartz powder in order to avoid temperature gradients in the catalyst bed. Prior to reaction, the catalyst was pre-treated with 20% O<sub>2</sub>/He at 573 K for 1 h to remove any possible impurities on the surface. The feed gas

composition is MeOH/O<sub>2</sub>/He = 5.5/10.6/83.9 (vol.%) and the typical gas hourly space velocity is 20,000 ml g<sub>cat</sub><sup>-1</sup> h<sup>-1</sup>. Methanol was introduced by bubbling He through a glass saturator filled with methanol and kept at 301 K, and it was then mixed with the 20% O<sub>2</sub>/He stream coming from a mass flow controller. The products were analyzed by an on line gas chromatograph (Agilent 6890N) equipped with TCD and FID detectors.

## 3 Results and Discussion

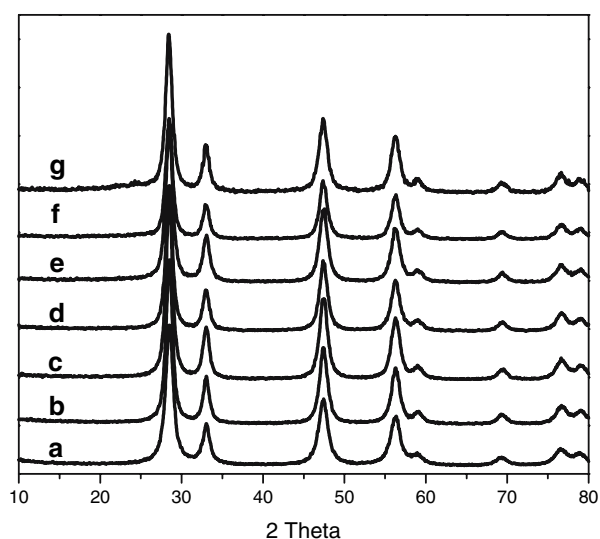
### 3.1 Physical and Chemical Features of the ReO<sub>x</sub>/CeO<sub>2</sub> Catalysts

Table 1 summarizes the physical and chemical parameters of the ReO<sub>x</sub>/CeO<sub>2</sub> catalysts. The surface areas decreased from 76 to 20 m<sup>2</sup> g<sup>-1</sup> as the loading of Re increased from 2.9 to 16.8 wt.%. Figure 1 shows the XRD patterns of the ReO<sub>x</sub>/CeO<sub>2</sub> catalysts. There were only typical diffractions of CeO<sub>2</sub> with fluorite structure (PDF no. 43-1002), and the average crystallize size of ceria was about 7 nm for all the samples. The absence of diffractions from ReO<sub>x</sub> suggests that rhenium oxides are well dispersed on ceria.

Figure 2 shows the H<sub>2</sub>-TPR profiles of the ReO<sub>x</sub>/CeO<sub>2</sub> catalysts. For CeO<sub>2</sub> alone, a weak and broad reduction peak at about 785 K was observed, representing the removal of surface oxygen [8]. However, the reduction peaks of the ReO<sub>x</sub>/CeO<sub>2</sub> catalysts were symmetrically shifted to 690–753 K. With increasing Re loading, the reduction temperature for the ReO<sub>x</sub>/CeO<sub>2</sub> catalysts gradually shifted to low region and reached the lowest value of 690 K at Re loading of 6.4 wt.%. It was previously proposed that the monolayer dispersion of ReO<sub>x</sub> corresponded to a surface coverage of about one Re atom per 0.35 nm<sup>2</sup> [9–12]. By considering the BET surface area of 64 m<sup>2</sup> g<sup>-1</sup>, the loading of 6.4 wt.% Re equaled to a Re surface density of one Re atom per 0.31 nm<sup>2</sup>, indicating the monolayer dispersion of ReO<sub>x</sub> on ceria. Further increasing Re loading, the reduction peaks shifted to higher temperature, probably due to the

**Table 1** Surface area and hydrogen consumption of the ReO<sub>x</sub>/CeO<sub>2</sub> catalysts

Re loading (wt.%)	S <sub>BET</sub> (m <sup>2</sup> g <sub>cat</sub> <sup>-1</sup> )	Re surface density/Re·nm <sup>-2</sup>	H <sub>2</sub> uptake (mmol g <sub>cat</sub> <sup>-1</sup> )	H <sub>2</sub> /Re ratio
2.9	76	1.2	0.6	3.8
4.7	69	2.2	0.9	3.6
6.4	64	3.2	1.2	3.5
9.0	60	4.9	1.6	3.3
12.7	34	12.1	2.2	3.2
16.8	20	27.2	2.8	3.1



**Fig. 1** XRD patterns of the  $\text{ReO}_x/\text{CeO}_2$  catalysts: (a)  $\text{CeO}_2$  and Re loading of (b) 2.9 wt.%, (c) 4.7 wt.%, (d) 6.4 wt.%, (e) 9.0 wt.%, (f) 12.7 wt.%, and (g) 16.8 wt.%

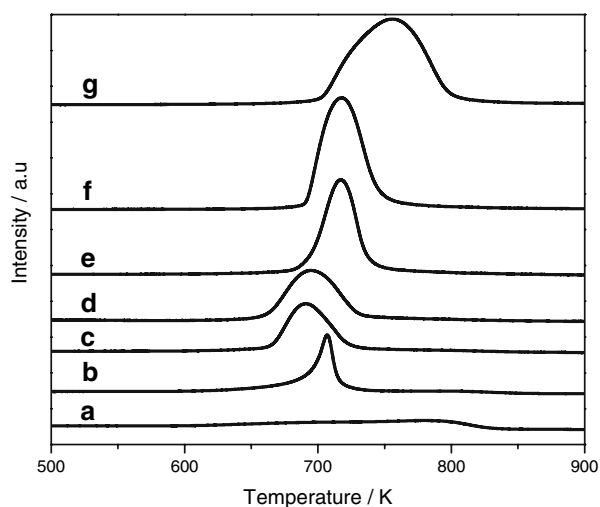


**Fig. 2** TPR profiles of the  $\text{ReO}_x/\text{CeO}_2$  catalysts: (a)  $\text{CeO}_2$  and Re loading of (b) 2.9 wt.%, (c) 4.7 wt.%, (d) 6.4 wt.%, (e) 9.0 wt.%, (f) 12.7 wt.%, and (g) 16.8 wt.%

formation of multilayered  $\text{ReO}_x$  species. Thus, it seems true that the monolayer dispersion of  $\text{ReO}_x$  on ceria is readily reducible. As shown in Table 1, the calculated moles of hydrogen consumed for the catalysts further demonstrated that the  $\text{H}_2/\text{Re}$  ratio decreased from 3.8 to 3.1 when Re loading increased from 2.9 to 16.8 wt.%, suggesting that the reduction mainly occurred on  $\text{ReO}_x$ .

### 3.2 Methanol Oxidation

Figure 3 shows the specific reaction rate and the product distribution of methanol oxidation over the  $\text{ReO}_x/\text{CeO}_2$

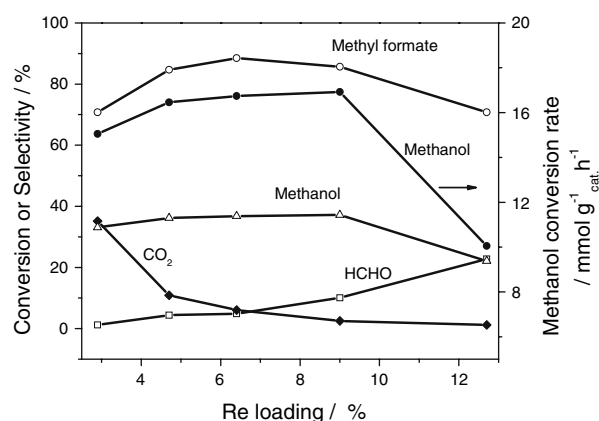


**Fig. 3** Effect of Re loading on the reaction rate of methanol and the selectivities of the products over the  $\text{ReO}_x/\text{CeO}_2$  catalysts. Reaction conditions: 513 K,  $\text{MeOH}/\text{O}_2/\text{He} = 5.5/10.6/83.9$  vol.%,  $\text{GHSV} = 20,000 \text{ ml g}_{\text{cat}}^{-1} \text{ h}^{-1}$

catalysts as a function of Re loading at 513 K. The reaction rate of methanol steadily increased with increasing Re loading and reached the maximum value of about  $17 \text{ mmol g}_{\text{cat}}^{-1} \text{ h}^{-1}$  at Re loading of 9 wt.%. Thereafter, the reaction rate of methanol significantly decreased to  $10 \text{ mmol g}_{\text{cat}}^{-1} \text{ h}^{-1}$  when the loading of rhenium further increased up to 12.7 wt.%. Formaldehyde, methyl formate, and carbon dioxide were detected as the main products. Dimethyl ether and dimethoxy methane were detected as minor products with total selectivity of  $<2.5\%$ . The selectivity of methyl formate increased with Re loading and reached the maximum value of 88.5% at 6.4 wt.% Re and then decreased slowly when the loading of Re is further increased. Carbon dioxide was the main by-product at low Re loading. The selectivity to carbon dioxide significantly decreased from 35 to 11% when the loading of Re increased from 2.9 to 4.7 wt.% and kept below 6% at higher loadings. The selectivity of formaldehyde increased with Re loading and become significant when Re loading exceeded 6.4 wt.%. Hence, it is apparent that there is a threshold of Re loading of 6.4 wt.% for the  $\text{ReO}_x/\text{CeO}_2$  catalysts, corresponding to the monolayer dispersion of  $\text{ReO}_x$  on  $\text{CeO}_2$ , where both the reaction rate of methanol and the selectivity of methyl formate could approach the most promising values.

Figure 4 shows the reaction rate of methanol and the product selectivity as a function of reaction temperature over the 6.4 wt.%  $\text{ReO}_x/\text{CeO}_2$  catalyst. The specific reaction rate of methanol initially increased from  $1.6 \text{ mmol g}_{\text{cat}}^{-1} \text{ h}^{-1}$  at 453 K to  $7.7 \text{ mmol g}_{\text{cat}}^{-1} \text{ h}^{-1}$  at 493 K, and then rapidly increased to  $22 \text{ mmol g}_{\text{cat}}^{-1} \text{ h}^{-1}$  at 533 K. Meanwhile, the selectivity of methyl formate kept at 80–90% in the whole temperature range, and the selectivity to formaldehyde was also relatively stable (4–6%). Dimethoxy

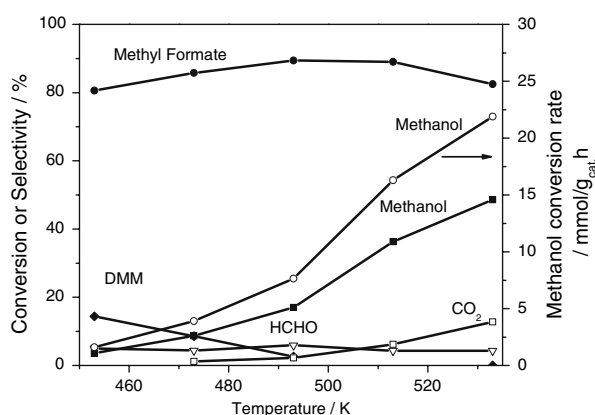


**Fig. 4** Effect of temperature on the reaction rate of methanol and the selectivities of the products over the 6.4  $\text{ReO}_x/\text{CeO}_2$  catalyst. Reaction conditions:  $\text{MeOH}/\text{O}_2/\text{He} = 5.5/10.6/83.9$  vol.%, GHSV =  $20,000 \text{ ml g}_{\text{cat}}^{-1} \text{ h}^{-1}$

methane was observed to be the main by-product (14.4%) at 453 K, and it practically disappeared at 513 K. Carbon dioxide became the main by-product (6%) at 513 K and it rapidly increased to 13% at 533 K.

Figure 5 shows the effect of contact time on the selectivities of the products over the 6.4 wt.%  $\text{ReO}_x/\text{CeO}_2$  catalyst at 513 K. The selectivity of methyl formate initially increased with contact time and reached maximum value of about 90% at 0.18 s, and then it decreased slightly with further increasing contact time. The selectivity of  $\text{CO}_2$  increased monotonously with contact time, while HCHO exhibited an opposite trend. Simultaneously, the reaction rate of methanol decreased remarkably with contact time which was  $29 \text{ mmol g}_{\text{cat}}^{-1} \text{ h}^{-1}$  at 0.045 s and  $16 \text{ mmol g}_{\text{cat}}^{-1} \text{ h}^{-1}$  at 0.18 s, respectively. Further

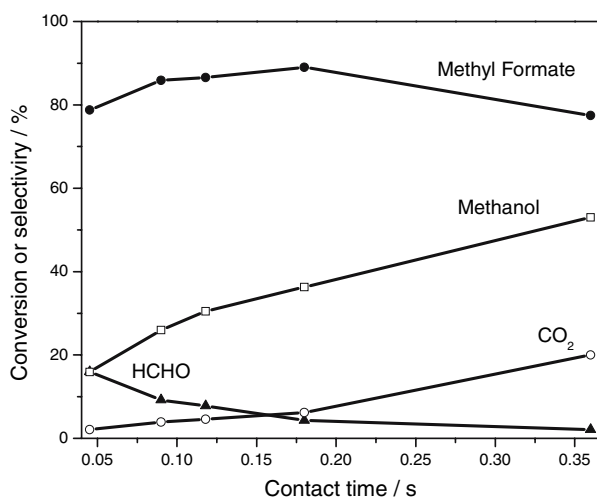


**Fig. 5** Effect of contact time on the selectivities of the products over the 6.4  $\text{ReO}_x/\text{CeO}_2$  catalyst. Reaction conditions: 513 K,  $\text{MeOH}/\text{O}_2/\text{He} = 5.5/10.6/83.9$  vol.%

increasing the contact time to 0.36 s, the reaction rate of methanol slightly decreased to  $12 \text{ mmol g}_{\text{cat}}^{-1} \text{ h}^{-1}$ .

The contact time dependence of formaldehyde and methyl formate suggests that HCHO is the primary product and methyl formate is produced by the reaction of the initially formed HCHO with methanol. On the other hand, the increase of  $\text{CO}_2$  selectivity with contact time and reaction temperature indicates that  $\text{CO}_2$  could be produced by the secondary reaction of methyl formate or other intermediates. Thus, it can be assumed that methyl formate was mainly produced through the etherification of adsorbed formate with methanol. However, the formation of dimethoxy methane by the condensation of methanol and formaldehyde would also take place at lower temperature, as shown in Fig. 4.

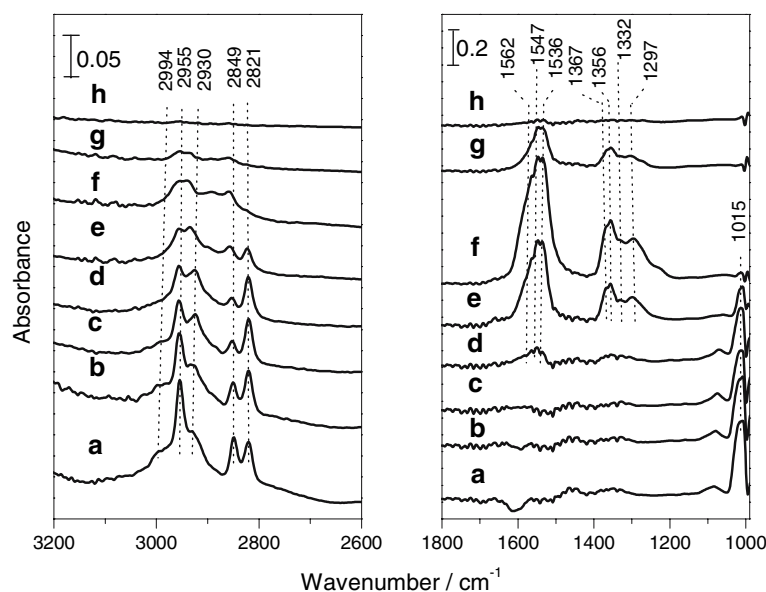
### 3.3 In situ FT-IR

#### 3.3.1 Methanol Adsorption

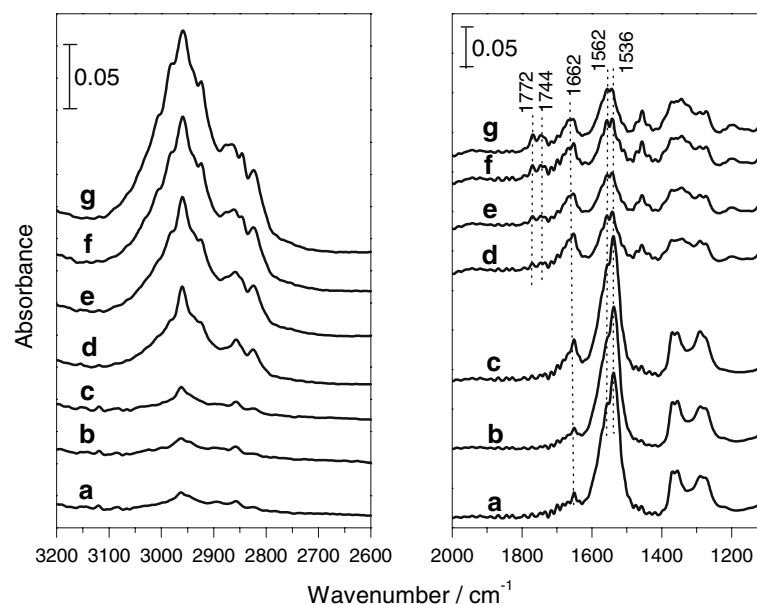
Figure 6 shows the IR spectra of adsorbed methanol on the 6.4 wt.%  $\text{ReO}_x/\text{CeO}_2$  catalyst. Upon adsorption at room temperature, surface  $-\text{OCH}_3$  species was readily formed by condensation of methanol with surface OH of the catalyst. The bands at  $2,930$  and  $2,821 \text{ cm}^{-1}$  corresponded to the bond vibration of  $\nu_s(\text{CH}_3)$  and the Fermi resonance of  $2\delta_s(\text{CH}_3)$ , respectively, in the methoxy group [5, 13–18]. The bands at  $2,955$  and  $2,849 \text{ cm}^{-1}$  could be assigned to the same mode occurring in the undissociatively adsorbed methanol. The weaker shoulder at  $2,994 \text{ cm}^{-1}$  was attributed to the asymmetric stretch ( $\nu_{\text{as}}$ ) of the  $\text{CH}_3$  species. The band at  $1,015 \text{ cm}^{-1}$  is a distinct absorption band of valence vibration  $\nu(\text{CO})$ . Upon heating under He flow, the absorption bands of the  $-\text{OCH}_3$  species significantly decreased and practically disappeared at 573 K. Absorption bands at  $1,562$ ,  $1,547$ ,  $1,536$ ,  $1,367$ ,  $1,356$ ,  $1,332$  and  $1,297 \text{ cm}^{-1}$ , which are characteristic of  $\nu_{\text{as}}(\text{COO}^-)$ ,  $\delta(\text{CH})$ , and  $\nu(\text{COO}^-)$  of formate complex appeared [5, 18], appeared at 423 K and attained their maximum intensities at 523 K, followed by rapid decrease and finally disappeared at 623 K. This phenomenon clearly indicates that the  $-\text{OCH}_3$  species was oxidized into formate species by the lattice oxygen of the catalyst. As increasing temperature higher than 523 K, the adsorbed formate species were further oxidized or decomposed to CO and  $\text{CO}_2$ .

Figure 7 shows the IR spectra of adsorbed methanol on the 6.4 wt.%  $\text{ReO}_x/\text{CeO}_2$  catalyst at 473 K and then purged with  $\text{CH}_3\text{OH}/\text{He}$  stream. As mentioned above, heating pre-adsorbed methanol on the catalyst to 473 K under He flow already produced formate species on the surface. When methanol was introduced, the absorption bands at  $1,562$  and  $1,536 \text{ cm}^{-1}$  representing adsorbed formate decreased

**Fig. 6** IR spectra of methanol adsorbed on the 6.4 ReO<sub>x</sub>/CeO<sub>2</sub> catalyst at room temperature (a) and purged with He at (b) 323 K, (c) 373 K, (d) 423 K, (e) 473 K, (f) 523 K, (g) 573 K, and (h) 623 K



**Fig. 7** IR spectra of methanol adsorbed on the 6.4 ReO<sub>x</sub>/CeO<sub>2</sub> catalyst at 473 K (a) and purged with MeOH/He stream for (b) 1 min, (c) 3 min, (d) 5 min, (e) 7 min, (f) 10 min, and (g) 15 min



gradually, and the absorption band at  $1,662\text{ cm}^{-1}$ , corresponding to undissociatively adsorbed methyl formate, slowly increased. After purging for 5 min, new absorption bands at  $1,744$  and  $1,772\text{ cm}^{-1}$ , which could be assigned to gaseous methyl formate, appeared and gradually increased with time on stream. Thus, it can be assumed that methanol was immediately dissociated into surface  $-\text{OCH}_3$  species, which could be easily oxidized into formate at  $473\text{ K}$  by the lattice oxygen of the catalyst. When purged with  $\text{CH}_3\text{OH}/\text{He}$ , the gaseous methanol reacted with the surface formate, resulting in the formation of gaseous methyl formate.

### 3.3.2 Formaldehyde Adsorption

Figure 8 shows the IR spectra of adsorbed formaldehyde on the 6.4 wt.% ReO<sub>x</sub>/CeO<sub>2</sub> catalyst. At room temperature, the absorption bands at  $1,635$ ,  $1,469$ , and  $1,275\text{ cm}^{-1}$  could be assigned to the vibrations of  $\nu(\text{C}=\text{O})$ ,  $\delta(\text{CH}_2)$ , and  $\gamma(\text{CH}_2)$  in adsorbed formaldehyde [13, 18, 19]. The formation of formate was identified by the absorption bands at  $1,546$  ( $\nu_{\text{as}}(\text{COO}^-)$ ) and  $1,374\text{ cm}^{-1}$  ( $\nu_{\text{s}}(\text{COO}^-)$ ). The adsorption bands at  $1,490$ ,  $1,408$ ,  $1,305$ ,  $1,229$ ,  $1,164$ , and  $1,114\text{ cm}^{-1}$  corresponded to  $\delta(\text{CH}_2)$ ,  $\omega(\text{CH}_2)$ ,  $\tau(\text{CH}_2)$ ,  $\gamma(\text{CH}_2)$ , and  $\nu(\text{CO})$  in dioxymethylene complex [5, 18]. The



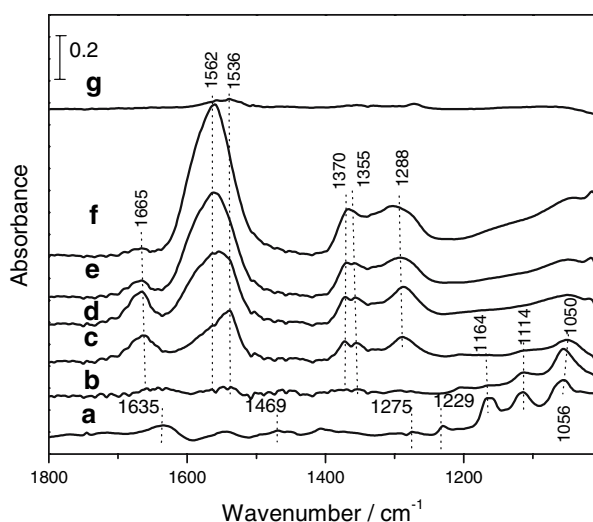


**Fig. 8** IR spectra of formaldehyde adsorbed on the 6.4  $\text{ReO}_x/\text{CeO}_2$  catalyst at room temperature (a) and purged with He at (b) 323 K, (c) 373 K, (d) 423 K, (e) 473 K, (f) 523 K, and (g) 573 K

presence of methoxy was also confirmed by the typical bands at 1,455 and  $1,056\text{ cm}^{-1}$ .

Upon heating under He flow, the bands belonging to adsorbed formaldehyde and dioxymethylene either disappeared or substantially decreased. New absorption bands at 1,665, 1,562, 1,355, and  $1,288\text{ cm}^{-1}$  appeared at 373 K. The bands at 1,665 and  $1,288\text{ cm}^{-1}$  could be assigned to the vibrations  $\nu(\text{C}=\text{O})$  and  $\nu(\text{C}-\text{O})$  of undissociatively adsorbed methyl formate [5], and the bands at 1,562 and  $1,355\text{ cm}^{-1}$  represented the vibration  $\nu_{\text{as}}(\text{COO}^-)$ , and  $\nu_{\text{s}}(\text{COO}^-)$  of formate complex. At 423 K, the distinct absorption bands of undissociatively adsorbed methyl formate attained their maximum intensities. The intensities of

the absorption bands due to the formate complex reached maximum at 523 K and practically disappeared at 573 K.

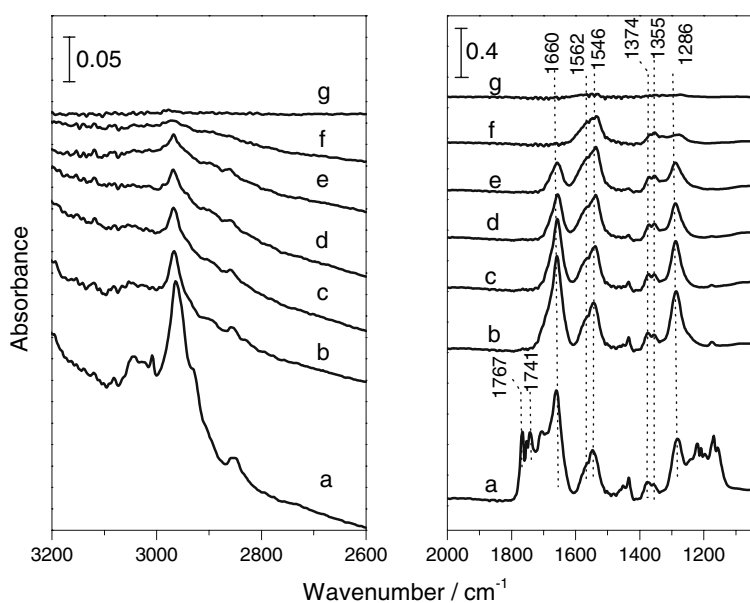
Hence, dioxymethylene was immediately produced once formaldehyde was adsorbed on the catalyst, evidencing that the formation of dioxymethylene was a rapid process even at room temperature. Dioxymethylene was then oxidized into formate species by lattice oxygen of catalyst at 423 K. Simultaneously, formaldehyde could produce methyl formate through dimerization. At higher temperature, methyl formate desorbed and formate species decomposed into CO and  $\text{CO}_2$ .

### 3.3.3 Methyl Formate Adsorption

Figure 9 shows the IR spectra of methyl formate adsorption on the 6.4 wt.%  $\text{ReO}_x/\text{CeO}_2$  catalyst. Upon adsorption at room temperature, both undissociatively adsorbed methyl formate with the characteristic bands at  $1,660\text{ cm}^{-1}$   $\nu(\text{C}=\text{O})$ ,  $1,452\text{ cm}^{-1}$   $\delta_{\text{as}}(\text{CH}_3)$ ,  $1,435\text{ cm}^{-1}$   $\delta_{\text{s}}(\text{CH}_3)$ ,  $1,286\text{ cm}^{-1}$   $\nu(\text{C}-\text{O})$  and  $1,173\text{ cm}^{-1}$   $\gamma(\text{CH}_3)$  and surface formate species with the typical bands at  $1,562\text{ cm}^{-1}$   $\nu_{\text{as}}(\text{COO}^-)$ ;  $1,374\text{ cm}^{-1}$ ,  $1,355\text{ cm}^{-1}$   $\nu_{\text{s}}(\text{COO}^-)$  were produced.

Upon heating under He flow, the absorption bands belonging to undissociatively adsorbed methyl formate rapidly decreased and practically disappeared at 523 K. On the other hand, the intensities of the absorption bands due to formate complex only slowly decreased and vanished at 573 K. It seems that the adsorbed methyl formate could decompose into surface formate species even at room temperature and the surface formate could further decompose to CO and  $\text{CO}_2$  at 523 K, similar to the case of formaldehyde adsorption.

**Fig. 9** IR spectra of methyl formate adsorbed on the 6.4  $\text{ReO}_x/\text{CeO}_2$  catalyst at room temperature (a) and purged with at (b) 323 K, (c) 373 K, (d) 423 K, (e) 473 K, (f) 523 K, and (g) 573 K



Therefore, the reaction network of methanol oxidation to methyl formate could be proposed as following. Adsorption of methanol produced surface methoxy species, which was then dehydrogenated to form formaldehyde as a rate-determining step. The adsorbed formaldehyde further reacted with gaseous methanol to form dimethoxymethane as a product or to form dioxymethylene species adsorbed on the surface of the catalyst. Dioxymethylene species could easily be oxidized into formate species by lattice oxygen, which would react with gaseous methanol to form methyl formate and/or would decompose into CO and CO<sub>2</sub>.

#### 4 Conclusion

Methanol selective oxidation to methyl formate could be efficiently performed over a ReO<sub>x</sub>/CeO<sub>2</sub> catalyst with Re monolayer dispersion. The specific reaction rate of methanol approached to 16 mmol g<sub>cat</sub><sup>-1</sup> h<sup>-1</sup> at 513 K with methyl formate selectivity of about 90%. Mechanistic studies with FT-IR further revealed that the formate species on the surface of the catalyst acted as the most important intermediate in the reaction network, which could react with gaseous methanol to form methyl formate and/or decompose into CO and CO<sub>2</sub>, depending on the reaction temperature.

#### References

1. Lee JS, Kim JC, Kim YG (1990) Appl Catal 57:1
2. Guerreiro ED, Gorris OF, Larsen G, Arrúa LA (2000) Appl Catal A 204:33
3. Jung KD, Joo OS (2002) Catal Lett 84(1–2):21
4. Guo YL, Lu GZ, Mo XH, Wang YS (2005) Catal Lett 99(1–2):105
5. Busca G, Elmi AS, Forzatti P (1987) J Phys Chem 91:5263
6. Forzatti P, Tronconi E, Busca G, Tittarelli P (1987) Catal Today 1:209
7. Ai M (1982) J Catal 77:279
8. Trovarelli A (1996) Catal Rev Sci Eng 38:439
9. Mol JC (1999) Catal Today 51:289
10. Xu YD, Wei XG, Shi YZ, Zhang YH, Guo XX (1986) J Mol Catal 36:79
11. Aldag AW, Lin CJ, Clark A (1978) J Catal 51:278
12. Yuan YZ, Iwasawa Y (2002) J Phys Chem B 106:4441
13. Busca G, Rossi PF, Lorenzelli V, Benoissa M, Travert J, Lavalley JC (1985) J Phys Chem 89:5433
14. Busca G, Lorenzelli V (1980) J catal 66:155
15. Burcham LJ, Briand LE, Wachs IE (2001) Langmuir 17:6164
16. Burcham LJ, Badlani M, Wachs IE (2001) J Catal 203:104
17. Locher V (2006) Appl Catal A 309:33
18. Locher V, Machek J, Tichý J (2002) Appl Catal A 228:95
19. Popova GY, Budneva AA, Andrushkevich TV (1997) React Kinet Catal Lett 61:353